

# Solid state $^1\text{H}$ NMR study, humidity sensitivity and protonic conduction of gel derived phosphosilicate glasses

N. J. Clayden,<sup>a</sup> S. Esposito,<sup>b</sup> P. Pernice<sup>c</sup> and A. Aronne\*<sup>c</sup>

<sup>a</sup>School of Chemical Science, University of East Anglia, Norwich, UK NR4 7TJ

<sup>b</sup>Laboratorio Materiali del Dipartimento di Meccanica, Strutture, Ambiente e Territorio, Facoltà di Ingegneria dell'Università di Cassino, Via G. Di Biasio 43, 03043 Cassino (Fr), Italy

<sup>c</sup>Department of Materials and Production Engineering, University of Naples Federico II Piazzale Tecchio, 80125 Napoli, Italy. E-mail: anaronne@unina.it

Received 20th June 2002, Accepted 10th September 2002

First published as an Advance Article on the web 16th October 2002

$^1\text{H}$  Magic Angle Spinning (MAS) NMR and  $^1\text{H}$   $T_1$  and  $T_{1\rho}$  relaxation times measurements were used to investigate structural aspects of gel derived glasses of composition  $10\text{P}_2\text{O}_5\cdot 90\text{SiO}_2$  (10P) and  $30\text{P}_2\text{O}_5\cdot 70\text{SiO}_2$  (30P), with the aim of understanding the different humidity sensitive behaviour observed for films of the same composition. The experimental evidence suggests that 10P and 30P gel samples heat treated at  $100^\circ\text{C}$  have a similar POH environment while further heating causes a different structural evolution of POH units. In particular, the 30P sample heat treated at  $400^\circ\text{C}$  shows a single  $^1\text{H}$  resonance while a number of resonances are seen in the  $^1\text{H}$  spectrum of the 10P sample heat treated at  $400^\circ\text{C}$ . Further evidence of the different structure of 10P and 30P samples was given by the NMR relaxation times measurements, the gels were found to be heterogeneous on a nanometric scale. Domains, about 60 nm in size, related to  $^1\text{H}$  resonance in POH were evenly distributed in the matrix of both gels, only in the 10P gel also larger domains (about 700 nm) were found that can be related to  $^1\text{H}$  resonance in SiOH groups. Finally, MAS in combination with variable temperature static NMR spectra provided detailed information on the network structural features present in the 30P sample heat treated at  $300^\circ\text{C}$  as well as in the 10P sample heat treated at  $400^\circ\text{C}$  and allowed investigation of the dynamic processes taking place in these samples.

## 1. Introduction

The characteristics of hydroxyl (OH) groups, both number and distribution, are important in determining the properties of glassy materials, in particular their proton conductivity. Studies on a variety of glasses including ultraphosphate,<sup>1,2</sup> phosphosilicate<sup>3</sup> and silicate<sup>4-6</sup> have indicated the presence of OH groups. In order to understand the relationship between the OH groups and any functional role it is necessary to characterise thoroughly the numbers of OH groups and their environment. Both  $^1\text{H}$  NMR and IR spectroscopy as well as NMR relaxation time measurements have played a vital part in discerning the nature of the hydroxyl environments. A detailed study by Mercier and co-workers<sup>1</sup> of the local structure of zinc ultraphosphate glasses combined  $^1\text{H}$  and  $^{31}\text{P}$  magic angle spinning (MAS) NMR measurements with one-dimensional  $^1\text{H}/^{31}\text{P}$  cross-polarisation (CPMAS) experiments, as well as spin lattice ( $T_1$ ) and spin-spin ( $T_2$ ) relaxation times. In this work, two different  $^1\text{H}$  NMR resonances were seen which were identified with OH groups associated with the two types of  $Q'_2$  unit present: corresponding to those bonded to  $\text{H}^+$  and those bonded to  $\text{Zn}^{+2}$  ( $Q'_n$ : the connectivity of the tetrahedral phosphorus with  $n$  the number of P-O-(P/Si) bonds). A third  $^1\text{H}$  NMR resonance was assigned to the presence of molecular water adsorbed on the glass surface.<sup>1</sup> The relaxation time measurements argued for a homogeneous distribution of the protons which are intimately connected to the  $Q'_2$  phosphate species.<sup>1</sup> Similarly Hosono *et al.* observed two different types of P-OH groups in lead and barium ultraphosphate glasses<sup>2</sup> by  $^1\text{H}$  MAS NMR and IR spectroscopy. These groups are involved in hydrogen bonds characterised by different

strengths.<sup>2</sup> Hydroxyl groups were also detected in phosphosilicate glasses containing 1–19 mol% of  $\text{P}_2\text{O}_5$  by Plotnichenko *et al.* using IR spectroscopy.<sup>3</sup> On the basis of the experimental IR data these authors proposed a model, supported by quantum-chemical methods, in which the OH groups in a phosphosilicate glass occur mainly in the form of  $(\text{Si-O})_3\text{-Si-OH}$  silanol centres and, for  $\text{P}_2\text{O}_5$  concentrations in excess of 2–3 mol%, the majority of these centres are hydrogen-bonded with non-bridging oxygen atoms of the  $(\text{Si-O})_3\text{P=O}$  phosphorus centres.<sup>3</sup> Eckert *et al.* on the other hand have investigated the effects of the water content on the synthetic and natural silicate glasses by  $^1\text{H}$  solid echo and  $^1\text{H}$  MAS NMR techniques.<sup>4</sup> In these glasses the water is present mainly as OH groups at low concentration (<2–4 wt%) while at higher concentrations molecular  $\text{H}_2\text{O}$  species dominate.<sup>4</sup> Moreover, they found that the total water content does not affect the linear dependence of  $^1\text{H}$  chemical shifts on the O-H...O distance, indicating that the hydrogen bonding characteristics of OH and  $\text{H}_2\text{O}$  species in the glasses are similar.<sup>4</sup> Evidence for hydrogen-bonded OH groups in silicate glasses was also observed by Zarubin using IR spectroscopy.<sup>5</sup>  $^1\text{H}$  MAS NMR spectroscopy was employed by Brus and Skrdlantova to investigate the structure of a hybrid siloxane network synthesised *via* a sol-gel method utilising different silicon molecular precursors with quartz powder as a filler of the resulting network.<sup>6</sup> They found that the number of methyl groups in the hybrid network strongly affects the dynamics of silanol protons. The siloxane network forms very thin layers at the surface of the quartz grains, the bridging oxygens of which are strongly hydrogen-bonded to the silanols and the water molecules of the network.<sup>6</sup>

An investigation of the attack of water on a sodium metaphosphate glass using  $^1\text{H}$  MAS NMR,<sup>7</sup> one- and two-dimensional  $^1\text{H}/^{31}\text{P}$  CP MAS<sup>7</sup> and radio frequency dipolar recoupled (RFDR) two-dimensional (2D) NMR exchange<sup>8</sup> experiments revealed a diversity of phosphate units, some connected through intra- and inter- molecular hydrogen bonds.<sup>7</sup> Tetrahedral phosphate species were also found by Alam and Lang originating from the dissolution of sodium phosphate glasses and their local spatial connectivity was examined.<sup>8</sup>

Phosphate glasses have found applications as fast proton conductors owing to their affinity towards water when either synthesised from oxides<sup>9</sup> or by using sol-gel methods.<sup>10–13</sup> Abe and co-workers proposed that an ionic type humidity sensing mechanism occurs in these gel derived glasses,<sup>11–13</sup> on the basis of conductivity measurements as a function of the temperature as well as of infrared (IR) absorption spectra. At low water content, chemical bonds form between the water molecules and the OH groups lying on the glass surface and the protons, dissociated from SiOH and/or POH bonds, move by hopping from the initial site to a neighbouring site. When these glasses contain water adsorbed in the pores, the proton conduction mechanism involves the proton transfer by hopping through water molecules. In addition they suggested that the proton conductivity is mainly controlled by the degree of hydrogen bonding. So the presence of the P=O bonds in the glass structure of the binary phosphosilicate glasses, by forming stronger hydrogen bonds, enhanced their proton transfer ability.<sup>12</sup>

Thin film phosphosilicate glasses have great potential as the sensing element in integrated humidity sensors. Indeed recent electrochemical impedance spectroscopic measurements have shown that amorphous films having the molar compositions  $10\text{P}_2\text{O}_5\cdot 90\text{SiO}_2$  (10P) and  $30\text{P}_2\text{O}_5\cdot 70\text{SiO}_2$  (30P) are very sensitive to humidity change.<sup>14</sup> In particular, the phosphorus content as well as the temperature of the heat treatments (100 and 300 °C) strongly affects the sensitivity to relative humidity (R.H.) of the gel derived films.<sup>14</sup>

In order to study the structural transformations that occur during the conversion from gel to gel derived glass in the above phosphosilicate glasses, a detailed  $^{29}\text{Si}$  and  $^{31}\text{P}$  MAS-NMR investigation was performed on bulk samples of these glasses for different heat treatments.<sup>15</sup> It was found that the 10P and 30P gels dried at 100 °C have very similar structures formed by a siloxane framework containing silanol groups and including isolated molecules of orthophosphoric acid and, a very small amount, of pyrophosphoric acid. In spite of this similarity, heating the gels of different composition to 300 °C caused radically different structural rearrangements of their glassy matrix. For the 10P gel only Si–O–Si bonds were formed, increasing the degree of polymerisation of the siloxane network, no evidence was seen for the formation of P–O–Si bonds. In marked contrast, P–O–Si bonds were formed after heating the 30P gel to the same temperature.<sup>15</sup> Additional 2D-NMR  $^{31}\text{P}$  magnetisation exchange experiments established that the 10P gel sample heated to 300 °C contained distinct domains, on the nanometre scale, of different phosphorus connectivity<sup>16</sup> since no magnetisation exchange was observed between  $Q'_2$ ,  $\text{OP}(\text{OP})_2(\text{OH})$ , with  $Q'_0$ ,  $\text{OP}(\text{OH})_3$ , and/or  $Q'_1$ ,  $\text{OP}(\text{OP})(\text{OH})_2$ , units, whereas an intense exchange process was noticed between  $Q'_0$  and  $Q'_1$  units, indicating a close association of these two structural units. A model for this association has been proposed involving a hydrogen bonded interaction between the  $Q'_0$  and  $Q'_1$  units.<sup>16</sup>

In this paper, the results of  $^1\text{H}$  NMR experiments on the 10P and 30P samples are reported with the aim of understanding why different proton conductivities are observed<sup>14</sup> for the glassy phases with the different phosphorus contents, 10 and 30  $\text{P}_2\text{O}_5$  mol%. A number of  $^1\text{H}$  NMR experiments were carried

out: high resolution  $^1\text{H}$  MAS NMR,  $^1\text{H}$   $T_1$  and  $T_{1\rho}$  relaxation times as well as low temperature  $^1\text{H}$  solid echo NMR.

## 2. Experimental

Phosphoryl chloride,  $\text{POCl}_3$ , (99%, Aldrich) and tetraethoxysilane,  $\text{Si}(\text{OC}_2\text{H}_5)_4$ , (99%, Gelest) (TEOS) were used as starting materials in the sol-gel preparation. Two compositions of phosphosilicate sols were prepared:  $10\text{P}_2\text{O}_5\cdot 90\text{SiO}_2$  (10P) gel and  $30\text{P}_2\text{O}_5\cdot 70\text{SiO}_2$  (30P) gel using a procedure that has been reported in a previous paper.<sup>14</sup> Complete gelation occurred at room temperature in 10 days for the 10P gel and in 14 days for the 30P gel. The gelled systems were held for one more day at room temperature before drying. The gels were fully dried in air at 100 °C in an electric oven for one day. After these treatments, transparent and amorphous bulk gel were obtained for both compositions. Thin films with thickness ranging from 0.8 to 1  $\mu\text{m}$  were also obtained for both compositions by means of a dip-coating procedure previously described.<sup>14</sup> Microscope slides as well as Corning (N. 7059) slides were used as substrates. Quantitative analysis of the phosphorus and silicon content in the gel derived glasses was performed for both gels.<sup>15</sup> The analysed compositions of the studied gels are in excellent agreement with the nominal composition showing that the synthetic procedure<sup>14</sup> significantly reduces the phosphorus loss in the gel derived glasses. Given this close agreement, the samples henceforth are labelled by their nominal compositions of  $\text{P}_2\text{O}_5$ . In addition, the qualitative evaluation of the phosphorus content in the film gel, performed using an EDS probe of a Leica Cambridge scanning electron microscopy (model S-240), also showed very good agreement with the nominal phosphorus content.

The electrical response of the films to the relative humidity (R.H.) was evaluated by electrochemical impedance spectroscopy using a Solartron 1260 impedance analyser. The lowest frequency used was 0.50 kHz to avoid polarisation at the film-electrode interface. The environments with a R.H. ranging from 20 to 86% were obtained by mixing dry and saturated air streams. The monitoring of R.H. within the test chamber was carried out using a hygrometric probe which gave results accurate to within  $\pm 2\%$ .

Before  $^1\text{H}$  NMR measurements the samples were heat treated at appropriate temperatures, allowed to equilibrate at 60% R.H. and then sealed in the sample holder. Solid state  $^1\text{H}$  NMR spectra were acquired on a Bruker MSL-200 NMR spectrometer operating at 200.13 MHz. NMR free induction decays (FID) of static samples were acquired using a solid echo pulse sequence  $[(\pi/2)_y - t_1 - (\pi/2)_x - t_2]$ , combined with phase cycling and an echo delay of 8  $\mu\text{s}$ , together with a pulse width of 3.0  $\mu\text{s}$ . A value of  $t_2$  was chosen to ensure that data acquisition began on the top of the solid echo. 4000 data points were acquired for the FID with a dwell time of 0.5  $\mu\text{s}$  to ensure a faithful reproduction of any fast decaying component. Static low temperature NMR spectra were obtained using the MAS probe with the temperature controlled by the Bruker variable temperature controller. Magic angle sample spinning (MAS) was carried out using a Bruker double bearing rotor system with 7 mm zirconia rotors and the NMR data collected using a single pulse excitation. Typical spinning speeds were 5 kHz, which was sufficient to make the spinning sidebands of low intensity and outside the region of interest. Ethanol was used as a secondary reference for the  $^1\text{H}$  chemical shifts, taking the methyl resonance as 1.16 ppm.

$T_1$  was measured using the saturation recovery method in a single point acquisition manner, collecting 256 points with a time increment of 10 ms, or 100 ms for the measurement of the long  $T_1$ . The  $T_{1\rho}$  decay was similarly obtained by single point acquisition with 256 points and a time increment of 200  $\mu\text{s}$  for the spin-locking pulse together with a spin-locking field of

83 kHz. A more accurate determination of the long  $T_{1\rho}$  was made by collecting the  $^1\text{H}$  NMR spectrum with spin-lock times of up to 400 ms. The rf amplitudes and phase orthogonality were checked prior to data acquisition using a standard multiple pulse tune up procedure on a  $\text{H}_2\text{O}$  sample. Typically the sample was left to equilibrate for one hour before collecting 32 transients. Experimental errors for use in the  $T_1$  and  $T_{1\rho}$  relaxation time analysis as well as the FID analysis were estimated from the last 20 data points of the appropriate data set. Non-linear least squares fitting based on the Levenberg–Marquardt algorithm was used to extract the  $^1\text{H}$  relaxation times from the appropriate decay curve and to function fit the FID. Spin diffusion experiments were carried out using the Goldman–Shen pulse sequence and a spin-lock preparatory period of 50 ms to allow for the decay of the short  $T_{1\rho}$  component.

### 3. Results and discussion

#### 3.1. Humidity sensitivity behaviour of the films

The sensitivity of the gel films towards humidity was evaluated by measuring the electrical impedance at different relative humidity at 20 °C. Microscope slides were used as the initial substrate for the impedance measurements with two parallel electrodes (5 mm distant) deposited on the film by sputtering. The film impedance is due to two effects: (1) the films bulk properties and its dependence on R.H. and (2) the electrode–film interface. The complex impedance plot of such a system may be schematically represented<sup>17</sup> by an equivalent circuit of two parallel resistance–capacitance loops in series giving two semi-circles on the impedance plot, Fig. 1. The two semi-circles can be partially overlapped depending on the resistance and capacitance values. The high frequency part of the impedance plots is representative of the film–R.H. interaction. We have measured the impedance only up to 0.50 kHz in order to avoid overlapping with electrode interface phenomena.

The electrical resistance ( $R_p$ ) of the films was calculated from the measured impedance values using a parallel resistance–capacitance equivalent circuit.<sup>17</sup> The  $R_p$  values of the 10P and 30P gel films, subjected to slow heating at 2 K  $\text{min}^{-1}$  up to 300 °C, changed markedly with relative humidity as shown in Fig. 2. The film resistance decreased as the relative humidity increased. These gel films contain a number of  $-\text{OH}$  groups<sup>14</sup> and physisorb water vapour. The water layer absorbed on the surface of the film allows a conductivity mechanism by protonic hopping.<sup>9</sup> The data in Fig. 2 also show that the behaviour of the film with respect to the R.H. was strongly affected by phosphorus content. Thus even if the 10P film was sensitive to the humidity, with behaviour quite similar to the 30P sample, its resistance was higher at all R.H. than the 30P film. This result suggests that the conductivity and the sensitivity to R.H. depend mainly on the  $-\text{OH}$  groups associated with phosphorous. However, the conductivity cannot

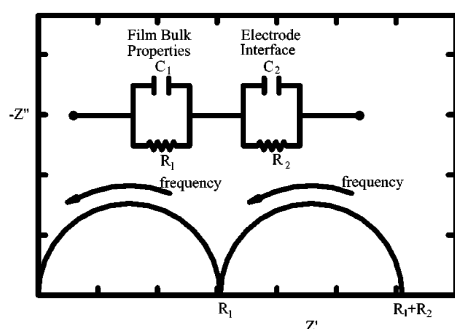


Fig. 1 Schematic complex impedance plot of the electrolytic film and its equivalent circuit.

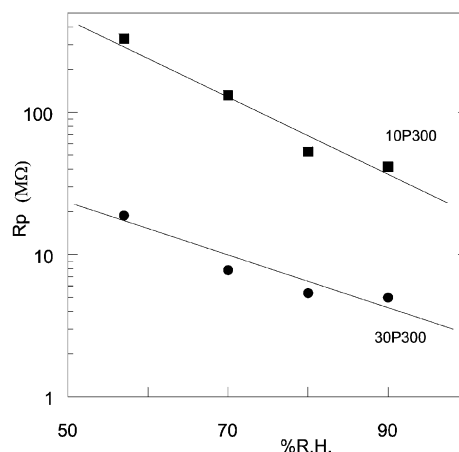


Fig. 2 The electrical resistance of the film containing 10 (10P) and 30 (30P) mol%  $\text{P}_2\text{O}_5$  heat treated at 300 °C.

be arbitrarily increased by further raising the phosphorous content in the gel because the chemical stability of the phases in the  $\text{SiO}_2$ – $\text{P}_2\text{O}_5$  binary system depend on the  $\text{P}_2\text{O}_5$  content. All attempts to increase the phosphorous content in the gel beyond 30 mol% failed as the gel was hygroscopic.

These results indicate that thin films in the  $\text{SiO}_2$ – $\text{P}_2\text{O}_5$  system are promising materials for humidity sensors. Thus, the presence of  $\text{SiO}_2$  makes for a stable and easily fabricated film, while  $\text{P}_2\text{O}_5$  gives the film its sensitivity to humidity. Although the low  $\text{P}_2\text{O}_5$  content of the 10P sample guarantees excellent chemical stability and reversibility, the resistance is too high for a practical device, especially at lower humidity. Consequently more extensive measurements were only carried out on the 30P composition. To lower the film resistance in order to allow the study of low R.H. values (below 20% R.H.), Corning slides (N. 7059) with a comb-type electrode, consisting of 10 fingers (5 mm length and 0.5 mm width) separated by gaps having the same width as the fingers, were used as the substrate. In Fig. 3(a), the complex impedance plots of a 30P film are reported. The d.c. film resistance value can be obtained from

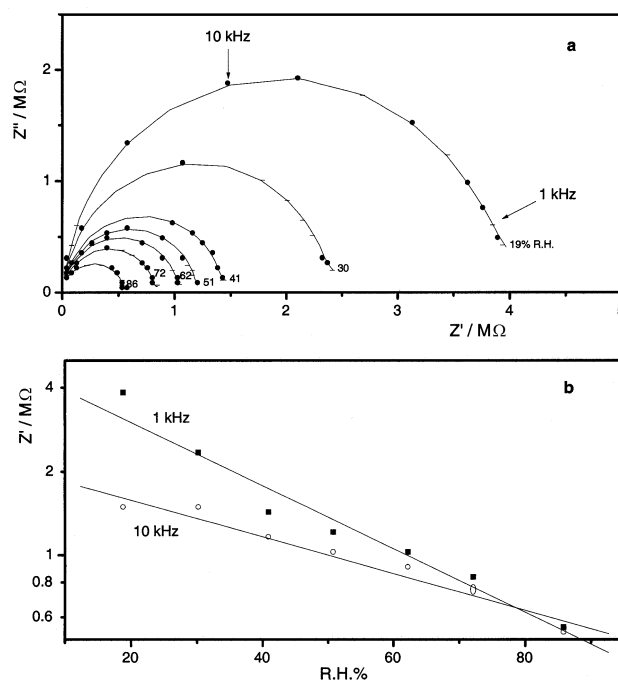


Fig. 3 (a) Complex impedance plots of the film containing 30 mol%  $\text{P}_2\text{O}_5$  heat treated at 300 °C; (b) real part of the impedance ( $Z'$ ) at 1 kHz and 10 kHz for different R.H. values.

the extrapolated diameter of each high frequency arc.<sup>17</sup> The change in the electrode geometry resulted in a lowering of the measured impedances and the data in Fig. 3(a) demonstrate that at 0.50 kHz the behaviour is almost purely resistive. The sensitivity of the film can be highlighted by plotting the real part of the impedance at a proper frequency without any processing of the impedance data. In Fig. 3(b) the real part of the impedance ( $Z'$ ) at 1 kHz and 10 kHz is plotted against the R.H. giving a linear trend.

Preliminary measurements of the response time to humidity change were also carried out for the 30P film. The response was very fast with increasing humidity but the return to low humidity was slow. This unusual behaviour seems to suggest that the water strongly interacts with the film during the absorption and that this process can not be described by a simple physisorption mechanism. In order to understand the different electric response to humidity change of the studied gel derived films as well as the type of interactions occurring between water and -OH groups, in the next section a detailed study of the -OH chemical environments by solid state  $^1\text{H}$  NMR is reported.

### 3.2. Solid state $^1\text{H}$ NMR measurements

$^1\text{H}$  NMR measurements were performed on 10P and 30P bulk gel samples heat treated at 100, 300, 400 and 1000 °C. These temperatures were selected on the basis of the earlier results.<sup>15</sup> Before each NMR experiment, samples were allowed to equilibrate with the environment R.H. (60%) to permit a proper comparison with the electrical response data. The room temperature  $^1\text{H}$  MAS NMR spectra of the heat treated 10P and 30P gels are shown in Fig. 4. In the NMR spectra of the samples heat treated to 100 °C three resonances are observed, two of which occur at the same chemical shift values ( $\delta = 1.06$  and 3.83 ppm) for both dried gels. These two resonances can be assigned to the methyl,  $\delta = 1.06$  ppm ( $\text{CH}_3\text{CH}_2\text{O}-$ ), and methylene,  $\delta = 3.83$  ppm ( $\text{CH}_2\text{CH}_2\text{O}-$ ), groups on the basis of their chemical shifts and relative integrals. This is also confirmed by the presence of  $^{13}\text{C}$  resonances in the  $^{13}\text{C}$  MAS NMR experiments consistent with ethoxy groups. The resonances at  $\delta = 7.4$  ppm (10P-100) and  $\delta = 8.9$  ppm (30P-100) are assigned to POH groups involved in weak hydrogen bonding.<sup>7</sup> No resonances attributable to SiOH groups (1.7–3 ppm) were seen. This is consistent with the greater sensitivity of Si–O–P bridges than Si–O–Si ones towards hydrolysis, under the experimental conditions utilised,<sup>14</sup> thus making the formation of POH terminal groups favoured over SiOH ones. At the same time, extensive hydrogen bonding of the POH groups is evident from the OH stretching frequency (*ca.* 3400  $\text{cm}^{-1}$ ) seen in the FTIR spectra of both dried gels.<sup>14</sup> The  $^1\text{H}$  NMR spectra of the dried gels are somewhat surprising since the presence of methyl and methylene  $^1\text{H}$  spin systems would, in a proton dense rigid lattice, lead to extremely broad lines, of the order of 10's kHz owing to the strong  $^1\text{H}$ – $^1\text{H}$  dipolar coupling. The spinning speeds used in the MAS experiments (5 kHz) would be insufficient to average such a homogeneous lineshape arising from multi-spin dipolar interactions of static methyl and methylene groups. However, two factors present in the studied system will contribute to the narrow resonances and hence high resolution  $^1\text{H}$  MAS NMR spectra. First, relative isolation of the ethoxy groups reducing the inter-group dipolar coupling and second motion of the groups, partially averaging the intra-group dipolar coupling. The somewhat broader resonances seen in the case of 10P would indicate in all likelihood that the dynamics are very slightly more constrained in this case, though the effect is marginal. These results together with the  $^{29}\text{Si}$ – $^{31}\text{P}$  MAS NMR data<sup>15</sup> that exclude the formation of P–O–Si bonds at this stage of the heat treatment, give a picture of the dried gels as a siloxane framework with trapped unreacted molecules of phosphoric and pyrophosphoric acid. The

chemical shifts seen for the POH ( $\delta = 7.4$  and 8.9 ppm for the 10P and 30P respectively) give an indication of the extent of hydrogen bonding, since as the hydrogen bonding becomes stronger so the proton becomes deshielded and the chemical shift becomes more positive. Therefore, in terms of the proposed interaction between the  $Q'_0$  and  $Q'_1$  units noted above the observed POH chemical shifts imply a stronger interaction between the  $Q'_0$  and  $Q'_1$  units in the 30P-100 siloxane network than in the 10P-100 sample.

The thermal analysis data show that the 10P and 30P gels behave in different ways on heating in air.<sup>14</sup> In the 10P gel, the residual organic groups evaporate without burning in the 280–350 °C temperature range, while in the 30P gel they burn in a lower temperature range, 230–320 °C. Consequently the  $^1\text{H}$  MAS NMR spectrum of the 10P sample, after heating to 300 °C, still exhibits the ethoxy group resonances whereas for the 30P-300 sample these resonances are greatly reduced in intensity indicating that, in this case, the thermal treatment forces the reaction further towards completion.<sup>14</sup> In addition the  $^1\text{H}$  MAS NMR spectrum of 10P-300 sample also shows substantial increases in linewidth attributable to a reduction in the ethoxy group dynamics, Fig. 4, and significant intensity can now be seen in the spinning sidebands. Therefore substantial changes in the correlation time of the ethoxy group dynamics must have occurred in the gel. In all likelihood the additional cross-linking of the silicate matrix seen in the  $^{29}\text{Si}$  MAS NMR spectrum<sup>15</sup> has resulted in a further constraint on the dynamics of the ethoxy groups. Nevertheless, for both samples heated to 300 °C a single narrow POH resonance is seen at  $\delta = 9.4$  ppm (10P) and  $\delta = 9.7$  ppm (30P), Fig. 4. A single type of POH environment seems implausible given the multiplicity of phosphorus resonances seen in the  $^{31}\text{P}$  MAS NMR spectra,<sup>15</sup> many of which have been shown to be proximal to protons by cross-polarisation experiments, together with the sensitivity of the POH chemical shift to the local hydrogen bonding environment. A possible explanation consistent with this observation is that fast chemical exchange is taking place between a number of POH environments leading to a single averaged chemical shift. On the other hand, although a narrow resonance may be indicative of a dynamic process and hence support the idea of chemical exchange, matters are not as clear cut in the case of the 30P-300 sample since a narrow resonance may just indicate that the remaining protons are isolated; particularly given the marked reduction in the intrinsic dipolar coupling with the loss of the ethoxy groups. However, strong evidence for the continued presence of some dynamic process is given by the  $^{31}\text{P}$  MAS NMR resonances<sup>15</sup> where the  $\delta = 0$  ppm ( $Q'_0$ ) and  $\delta = -12$  ppm ( $Q'_1$ ) of the 30P-300 sample are substantially narrowed. Therefore, the single narrow  $^1\text{H}$  NMR resonance strongly suggests a fast dynamic equilibrium between different phosphorus sites. It is worth emphasising that for both compositions the siloxane framework is highly cross-linked and the mobile species are presumably trapped molecular species within this matrix. For the 30P-300 sample, the higher phosphorus content gives rise to an even more highly cross-linked siloxane framework and simultaneously forces the silicon to go into six-fold coordination producing high connectivity phosphorus molecular species ( $\text{PO}_4$  tetrahedra with all bridging oxygen).<sup>15</sup>

Heating the 30P sample to 400 °C causes a further decrease in the intensity of the residual ethoxy group resonances while the POH resonance shifts marginally to 9.37 ppm, Fig. 4. Again only a single narrow resonance is seen. In marked contrast, when the 10P sample is heated to 400 °C a number of resonances are seen; the one at 0.5 ppm is assigned to isolated  $\text{SiOH}^4$  and those between 9.9 ppm and 6.6 ppm to POH groups in different environments.<sup>18</sup> The assignment of the resonance at 0.5 ppm is not clear cut since it lies outside the expected range for SiOH seen in aluminosilicates and silica gels.<sup>19</sup> However, the proton chemical shift in a silanol is known to be sensitive to

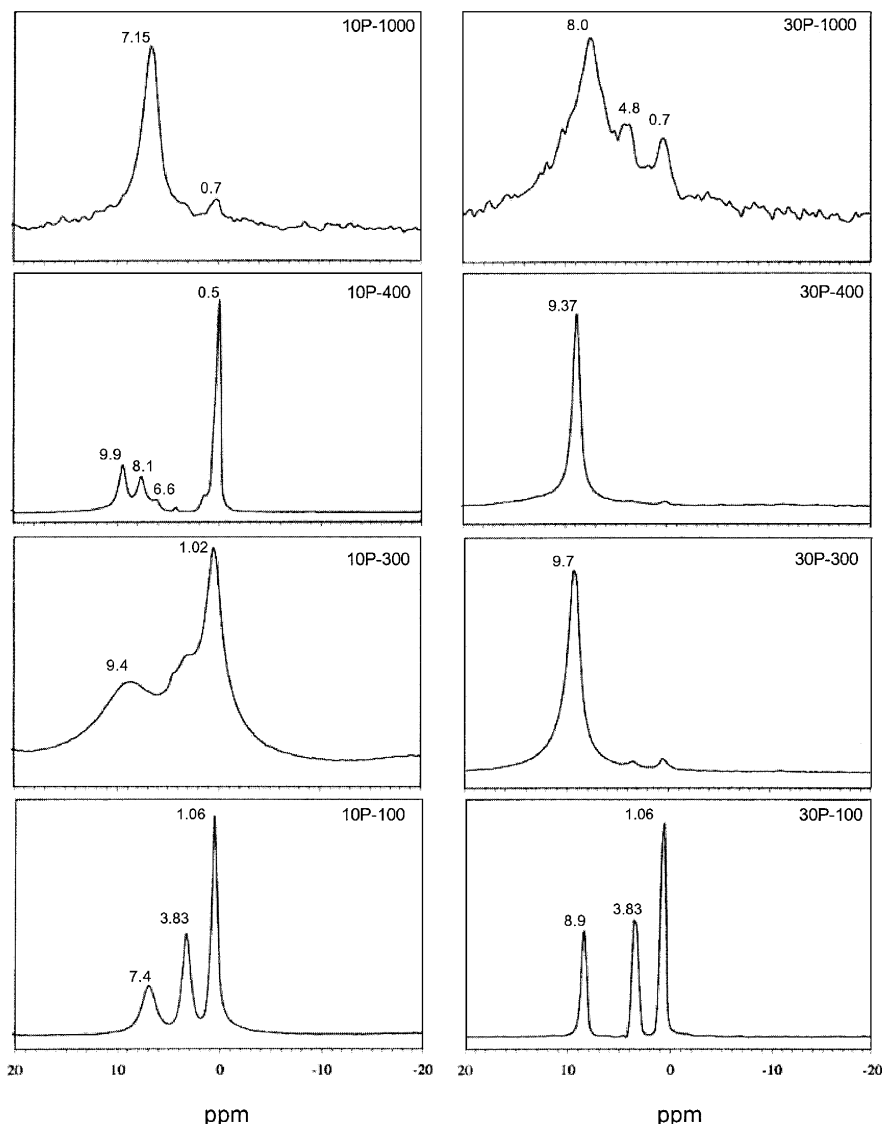


**Fig. 4**  $^1\text{H}$  MAS NMR spectra of the gels containing 10 (10P) and 30 (30P) mol%  $\text{P}_2\text{O}_5$  at different stages of heat treatment. The heat treated samples were collected under identical conditions, with a long enough H-1 relaxation delay so all are at thermal equilibrium. The spectra are plotted to a common peak height for ease of comparison. The normalised peak heights for the 10P samples are: 1.0 (100 °C); 0.40 (300 °C); 0.68, (400 °C); 0.002 (1000 °C); and for the 30P samples are: 1.0 (100 °C); 0.62 (300 °C); 0.05 (400 °C); 0.02 (1000 °C).

the hydrogen bonding and one possibility is that the proton is an extremely isolated SiOH, not involved in any hydrogen bonding. Support for this idea is provided by the  $^1\text{H}$   $T_1$  and  $T_{1\rho}$  data presented below. An alternative assignment to a methyl group can be ruled out on the basis of a  $^{13}\text{C}$  MAS NMR spectrum which showed no methyl resonances. At the same time as these differences in the  $^1\text{H}$  NMR spectra are seen, so different types of cross-linking are observed in the  $^{29}\text{Si}$  and  $^{31}\text{P}$  NMR spectra. After heating to 400 °C the 10P sample is still amorphous whereas an early stage of crystallisation has taken place in the 30P sample.<sup>15</sup> Although the nature of the crystallising phase cannot be identified unambiguously, a clear candidate is the hydrous analogue of  $\text{SiP}_2\text{O}_7$ , which contains only six-coordinated silicon atoms.<sup>15</sup> In such a phase the higher connectivity of the silicophosphate network precludes the presence of silanol groups and indeed, consistent with this interpretation, no silanol type resonances are seen in the 30P-400  $^1\text{H}$  MAS NMR spectrum, Fig. 4.

After heating the 10P and 30P gels to 1000 °C the  $^1\text{H}$  signal intensity decreases markedly, Fig. 4, with only a low intensity POH resonance at around 7–8 ppm. In addition, the low intensity of the  $\sim 0.5$  ppm resonance in the spectrum of the 10P-1000 sample suggests that finally the residual terminal SiOH have reacted and cross-linked. The additional resonance

at  $\delta = 4.7$  ppm for the 30P-1000 sample may represent absorbed water.<sup>4,6</sup>

In order to help understand the different humidity response of 10P and 30P films, the  $^1\text{H}$   $T_1$  and  $T_{1\rho}$  NMR relaxation times of the heat treated gel derived samples were also measured. The NMR relaxation times allow the  $^1\text{H}$  dynamics as well as the heterogeneity of the  $^1\text{H}$  spins to be determined. Dynamic processes, by modulating the dipolar coupling, give rise to variations in the observed  $T_1$  and  $T_{1\rho}$ . Although in principle the relaxation times allow the motions of the  $^1\text{H}$  spins to be modelled this is not straightforward when relaxation times can only be measured over a small temperature range, as in this case. Despite this, if the relaxation times are short, qualitative conclusions can be drawn about the importance of dynamics at the appropriate frequency, MHz and kHz for  $T_1$  and  $T_{1\rho}$ , respectively. Owing to the V-shaped relationship between  $T_1$ ,  $T_{1\rho}$  and the correlation time for the dynamics, long relaxation times may indicate either fast or slow dynamics. In a heterogeneous material where a  $^1\text{H}$  nuclear spin may experience differences in dipolar coupling and dynamics we can expect a characteristic relaxation time for each environment. However, the observation of these unique relaxation times will depend on whether they are averaged or not by a process known as spin

diffusion. A single averaged time will be seen if the phases are sufficiently close for the magnetisation to diffuse between them in a time of the order of the relaxation time. For three-dimensional diffusion this is described by the relationship<sup>20</sup>

$$d = \sqrt{6D_s T_{1,\rho}}$$

where  $d$  indicates the size of the domain. When spin diffusion is present the observation of a multi-exponential decay is best regarded only in qualitative terms as being indicative of phase heterogeneity on a particular distance scale. Quantification of the contributing phases and their dynamics is complex.

To avoid any confounding effect on the NMR relaxation times from the ethoxy group which is not relevant to the proton mobility, the room temperature  $^1\text{H}$   $T_1$  and  $T_{1\rho}$  NMR relaxation times were only measured for those samples free from residual organics, namely the 10P-400, 30P-300 and 30P-400 samples, Table 1. For the 30P samples heated at 300 and 400 °C two components were seen for  $T_{1\rho}$  but only a single  $T_1$  was seen, Table 1. Only qualitative domain sizes can be derived since the spin diffusion coefficient for the system under study is not known with any accuracy. An estimate of  $1 \times 10^{-17} \text{ m}^2 \text{ s}^{-1}$  can be made based on a typical spin diffusion coefficient,  $D_s$ , of  $4 \times 10^{-16} \text{ m}^2 \text{ s}^{-1}$ , seen for polymers where the dipolar coupling is of the order of 40 kHz<sup>20</sup> together with the observed room temperature linewidth of *ca.* 1 kHz, assuming this arises solely from dipolar coupling. The single  $T_1$  of around 0.4 s is then indicative of any phases present having a size of less than 200 nm. The 30P-300 and 30P-400 samples are therefore homogeneous on the 200 nm scale. Nevertheless in these samples some heterogeneity is revealed by the presence, in roughly equal amounts, of the two components  $T_{1\rho}$  that mainly differ in the long  $T_{1\rho}$  component, Table 1. Given the longer  $T_{1\rho}$  of 42.5 ms the size of these phases must be on the 60 nm scale. However, since only a single  $^1\text{H}$  resonance is seen in the respective MAS NMR spectra, Fig. 4, the chemical compositions would appear to be identical in terms of the  $^1\text{H}$  spins. The phases present must only represent variations in the dynamics of the  $^1\text{H}$  spins, perhaps related to the amount of adsorbed water. Therefore the 30P samples contain  $^1\text{H}$  phases with a domain size on the 60 nm scale. In marked contrast the 10P sample showed two distinct  $T_1$ , one very long one and one similar to the 30P sample, Table 1. In order to see such a long  $T_1$  component separately this phase must be of the order of 700 nm in size. Hence the 10P sample contains relatively large domains of a phase with a long  $^1\text{H}$   $T_1$ . The long  $T_1$  would indicate either a  $^1\text{H}$  spin remote from other spins or one with extreme dynamics: fast or slow. Confirmation of this is provided by the  $T_{1\rho}$  where again two components are seen in the same proportion as the  $T_1$  results. The phase present in greater amount again has a very long relaxation time, Table 1. To identify whether a specific  $^1\text{H}$  resonance gives rise to the particular relaxation times the  $^1\text{H}$  NMR spectra were acquired under selective conditions to see only the short  $T_1$  component and long  $T_{1\rho}$  component respectively. In the saturation recovery  $^1\text{H}$  NMR spectrum after a short recovery period of

50 ms only the resonances between 6 and 9 ppm were seen, while in the spin-locked  $^1\text{H}$  NMR experiment with a spin-lock of 100 ms only the resonance at 0.5 ppm was seen. These experiments conclusively demonstrate that the phases giving rise to the particular relaxation times are unique: the 0.5 ppm phase has a long  $T_1$  and  $T_{1\rho}$  while the 6–10 ppm resonances have short  $T_1$  and  $T_{1\rho}$ . Further evidence for the isolation of the two phases seen in the  $T_{1\rho}$  experiment for 10P-400 is provided by the Goldman–Shen experiment, where no spin diffusion was seen despite a recovery time of 1 s.

In order to confirm the above description of the nano-structure of the 30P-300 and 10P-400, and to investigate whether chemical exchange was taking place, variable temperature  $^1\text{H}$  static NMR spectra of 30P-300 and 10P-400 were acquired, shown in Figs. 5 and 6, respectively. In the case of the 30P sample, broadening of the single resonance started around 200 K, Fig. 5. Further broadening took place as the temperature was lowered until 160 K, when a resonance with a full width at half height (FWHH) in excess of 30 kHz was seen, Fig. 5. Such a large resonance linewidth can only arise from strong dipolar coupling involving  $^1\text{H}$  spins close together, as in  $\text{H}_2\text{O}$ . Clearly there must be significant  $^1\text{H}$  dynamics to average the large  $^1\text{H}$ – $^1\text{H}$  dipolar coupling and these dynamics must have an appreciable frequency and amplitude around 200 K. At no time during the temperature dependence was there any evidence for the freezing of chemical exchange in a slow exchange limit. The explanation for this is that, although the sample does contain different OH types, dynamic averaging is taking place through proton hopping. It is not plausible to have a single OH type given the variety of phosphorus environments close to  $^1\text{H}$  spins revealed by the  $^{31}\text{P}$  CP NMR results and the observation of more than one resonance in the 10P-400 sample. Thus the sample does indeed contain different OH types but the dynamic process giving exchange at high temperature is the same as the one averaging the dipolar coupling. At low temperature the chemically inequivalent resonances cannot be resolved in the broad dipolar broadened resonance. This is consistent with the relative rates; a rate of only  $1000 \text{ s}^{-1}$  would be enough to give fast exchange and only one resonance, while to average the dipolar coupling the rate must be in excess of  $50000 \text{ s}^{-1}$ . It should be noted that, from the point of view of these phases acting as proton conductors, these observations are consistent with the idea of a fast proton hopping between different POH sites.

Overall a similar picture is seen for the 10P-400 sample as the temperature is lowered but with one marked difference. At all

**Table 1**  $^1\text{H}$   $T_1$  and  $T_{1\rho}$  NMR relaxation times of the heat treated gel derived samples

Sample	$T_1$		$T_{1\rho}$	
	F	$T_1(\text{s})$	F	$T_{1\rho}(\text{ms})$
10P-400	0.38	0.56	0.39	4.43
	0.62	6.25	0.61	263.0
30P-300	1.0	0.42	0.50	5.71
	—	—	0.50	42.54
30P-400	1.0	0.35	0.32	5.35
	—	—	0.68	32.25

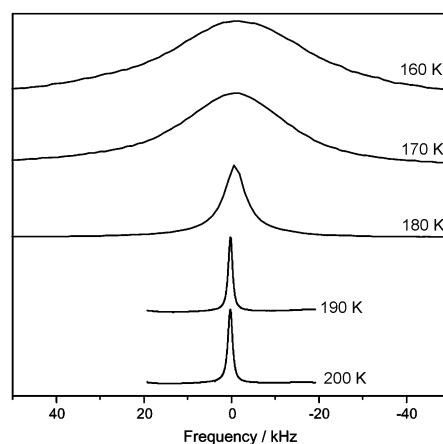


**Fig. 5** Variable temperature  $^1\text{H}$  static NMR spectra of the gel containing 30 mol%  $\text{P}_2\text{O}_5$  (30P) heat treated at 300 °C. 200.13 Hz corresponds to 1.0 ppm. Spectra at the different temperatures are plotted to a common peak height. The normalised peak heights are: 1.0 (200 K); 1.0 (190 K); 0.17 (180 K); 0.04 (170 K); 0.03 (163 K).

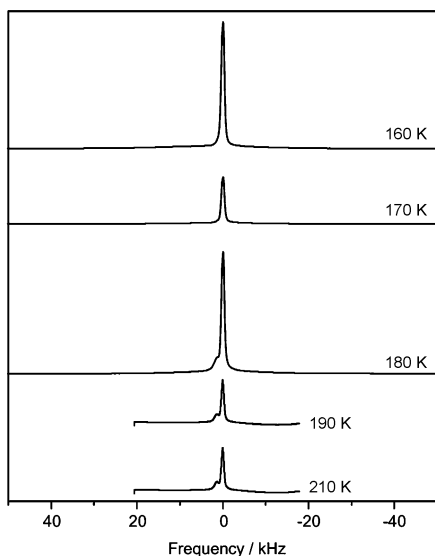


**Fig. 6** Variable temperature  $^1\text{H}$  static NMR spectra of the gel containing 10 mol%  $\text{P}_2\text{O}_5$  (10P) heat treated for 30 min at  $400\text{ }^\circ\text{C}$ .  $200.13\text{ Hz}$  corresponds to  $1.0\text{ ppm}$ . The peak heights above reflect the true peak heights.

temperatures the resonance at  $\sim 0\text{ ppm}$  shows only a small increase in its linewidth despite the changes in the other resonance, Fig. 6. This confirms the assignment of this resonance to an isolated  $\text{SiOH}$ . The resonances between 6 and 10 ppm broaden and show heterogeneous behaviour. At around  $200\text{ K}$ , whilst there is still a relatively sharp peak of *ca.*  $2\text{ kHz}$ , a broad foot appears about  $10\text{ kHz}$  wide. This shows that the dynamics are being frozen out in some regions whilst in others the  $^1\text{H}$  spins are still mobile. At  $180\text{ K}$  the foot is more pronounced,  $19\text{ kHz}$  wide, but still the resonance lying on top of it is only about  $2\text{ kHz}$  wide. Finally at  $160\text{ K}$  this foot disappears. Thus the 10P-400 sample not only shows chemical shift heterogeneity but also dynamic heterogeneity.

### 3.3. Protonic conductivity in gels

The above results are consistent with the different sensitivities toward humidity shown by the investigated gel derived films.  $^1\text{H}$  chemical shift is correlated with the  $\text{OH}\cdots\text{O}$  bond distance, *i.e.* with the strength of the hydrogen bonding,<sup>1,4</sup> an increase of the hydrogen bond strength increases the chemical shift value. Mercier *et al.*<sup>1</sup> found in ultraphosphate glasses a chemical shift  $\delta = 17\text{ ppm}$  for strong  $\text{P-O}\cdots\text{H-O-P}$  and  $\delta = 13\text{ ppm}$  for  $\text{PO-H}\cdots\text{H-OP}$  or  $\text{PO-H}\cdots\text{O=P}$ . These values of the chemical shift correspond,<sup>2</sup> respectively, to the IR band at  $2300$  and  $2900\text{ cm}^{-1}$ . Both compositions of our gel contain domains with P-OH acidic groups and absorbed water while  $^1\text{H}$  resonances are seen at values indicating weaker hydrogen bonding than in the above ultraphosphate glasses. The values of the chemical shift observed in our gel are only a little higher than those seen for  $\text{H}_3\text{O}^+$  in concentrated acidic solution.<sup>21</sup> Furthermore, a  $^1\text{H}$  resonance with a chemical shift of  $7.6\text{--}8.6\text{ ppm}$  was found by Mercier *et al.*<sup>18</sup> in ultraphosphate glasses interacting with humid air and attributed to the formation, on the glass surface, of concentrated phosphoric acid solution. The above values are anyway higher than the chemical shift value typical of water (about  $\delta = 5\text{ ppm}$ ), indicating therefore stronger hydrogen bonding than in water. On the other hand, the NMR relaxation times indicate that the gels are heterogeneous and that in the case of the 10P sample, the P-OH domains are more widely separated in the silicate matrix than in 30P. In both samples the P-OH groups act as active sites for water absorption allowing strong hydrogen bonding. The absorbed water molecules, as

they are rather tightly involved in hydrogen bonding, are not free to rotate and they can be supposed to be in an ice-like structure. It is this ice-like structure which provides a continuous pathway for fast proton hopping and the resulting proton conductivity within the P-OH domains. Critically the nature of the ice-like structure will depend on the OH groups content and distribution, as well as on the absorbed water linked by hydrogen bonds. In the usual view of proton conductivity, the proton hops in a concerted way through a whole array of water molecules (the relay mechanism).<sup>22</sup> By this mechanism it is easy to understand why in ice the observed proton mobility is higher than in water. Very fast proton conductivity is allowed whenever there is an ordered network of hydrogen bonds, as in some acidic salts, such as  $\text{CsHSO}_4$ .<sup>23</sup> The fast proton hopping in our gel also accounts for dynamic averaging of the different OH types and for the removal of the strong dipolar coupling seen until low temperature.

All the above considerations refer to the proton conductivity in the phosphorus-containing domains but it is noteworthy that the studied gels are heterogeneous also from the point of view of the electrical conductivity. In fact they are made up of conductive nanoparticles containing P-OH groups randomly dispersed in a nonconductive matrix. As a consequence, electrical conduction is possible only if continuous pathways of conductive particles are allowed. In such heterogeneous materials the conductivity increases with the volume fraction of the conductive phase. In these gels the conductive particles have the same size irrespective of the phosphorous content therefore, in comparison with 10P, the higher phosphorous content present in the 30P sample leads to a higher number POH conductive domains and so to a higher conductivity.

## 4. Conclusion

Solid state  $^1\text{H}$  MAS NMR with  $^1\text{H}$   $T_1$  and  $T_{1\rho}$  relaxation times as well as low temperature  $^1\text{H}$  solid echo NMR measurements have been performed on the 10P and 30P gel derived glasses in order to elucidate the different sensitivities toward humidity shown by the 10P and 30P gel derived films. Actually, the gel films show protonic conduction and for each R.H. value tested the 30P film has shown a lower electrical resistance than the 10P one.

From the NMR spectra it was found that a narrow single  $^1\text{H}$  resonance connected with POH groups was displayed by the 30P heat treated samples as a consequence of the fast chemical exchange occurring between different chemical environments. On the contrary,  $^1\text{H}$  resonances connected with isolated SiOH as well as with POH groups having different chemical environments were found in the 10P sample heated at  $400\text{ }^\circ\text{C}$  even if, for this composition, the samples heated at  $100$  and  $300\text{ }^\circ\text{C}$  have shown a behaviour similar to that of the 30P corresponding samples. The different behaviour on heating mirrors the different microstructure of the 10P and 30P heat treated samples. For both gel compositions the microstructure appears inhomogeneous and can be described as formed by domains having different sizes. In the 30P gel the domains size is on the  $60\text{ nm}$  scale with uniform distribution. On the contrary, in the 10P gel large domains ( $700\text{ nm}$ ) containing SiOH and small domains ( $60\text{ nm}$ ) including POH groups were found. In 30P the uniform distribution of small domains gives rise to dynamic processes producing chemical exchange between the POH with different environments, unlike 10P where different  $^1\text{H}$  resonances were found.

Both studied gels are humidity sensitive with a resistance decreasing with relative humidity. The different behaviour is consistent with the heterogeneous microstructure of the gels and with the sensitivity mechanism.

## Acknowledgements

The work was supported on behalf of National Research Council of Italy (CNR), Targeted Project "Special Materials for Advanced Technologies II" (No.980014 PF34).

## References

- 1 C. Mercier, L. Montagne, H. Sfihi, G. Palavit, J. C. Boivin and A. P. Legrand, *J. Non-Cryst. Solids*, 1998, **224**, 163.
- 2 H. Hosono, Y. Abe and K. Deguchi, *J. Non-Cryst. Solids*, 1992, **142**, 103.
- 3 V. G. Plotnichenko, V. O. Sokolov, E. B. Kryukova and E. M. Dianov, *J. Non-Cryst. Solids*, 2000, **270**, 20.
- 4 H. Eckert, J. P. Yesinowski, L. A. Silver and E. M. Stolper, *J. Phys. Chem.*, 1988, **92**, 2055.
- 5 D. P. Zarubin, *Phys. Chem. Glasses*, 1999, **40**, 184.
- 6 J. Brus and M. Skrdlantova, *J. Non-Cryst. Solids*, 2001, **281**, 61.
- 7 R. M. Wenslow and K. T. Mueller, *J. Phys. Chem. B*, 1998, **102**, 9033.
- 8 T. M. Alam and D. P. Lang, *Chem. Phys. Lett.*, 2001, **336**, 385.
- 9 Y. Abe, H. Hosono and O. Akita, *J. Electrochem. Soc.*, 1994, **141**, L64.
- 10 Y. I. Park, J. D. Kim and M. Nagai, *J. Mater. Sci. Lett.*, 2000, **19**, 2251.
- 11 C. Wang, M. Nogami and Y. Abe, *J. Sol-Gel Sci. Technol.*, 1999, **14**, 273.
- 12 M. Nogami, C. Wang and Y. Abe, Fast proton conducting P<sub>2</sub>O<sub>5</sub>-SiO<sub>2</sub> glasses, in *Proc. XVIII Cong. On Glass*, ACS, San-Francisco, 1998, vol. D3, pp. 139–144.
- 13 M. Nogami, R. Nagao, C. Wang and Y. Abe, *J. Sol-Gel Sci. Technol.*, 1998, **13**, 933.
- 14 M. D'Apuzzo, A. Aronne, S. Esposito and P. Pernice, *J. Sol-Gel Sci. Technol.*, 2000, **17**, 247.
- 15 N. J. Clayden, S. Esposito, P. Pernice and A. Aronne, *J. Mater. Chem.*, 2001, **11**, 936.
- 16 N. J. Clayden, S. Esposito and A. Aronne, *J. Chem. Soc., Dalton Trans.*, 2001, **13**, 2003.
- 17 J. R. MacDonald, *Impedance spectroscopy, emphasizing solid materials and systems*, John Wiley & Sons, New York, 1987, p. 25.
- 18 C. Mercier, L. Montagne, H. Sfihi and G. Palavit, *J. Non-Cryst. Solids*, 1999, **256–257**, 12.
- 19 G. Engelhardt and D. Michel, *High-Resolution Solid-State NMR of Silicate and Zeolites*, John Wiley & Sons, New York, 1986.
- 20 K. Schmidt-Rohr and H. W. Spiess, *Multidimensional Solid-State NMR and Polymers*, Academic Press, London, 1994.
- 21 C. I. Ratcliffe, J. A. Ripmeester and J. S. Tse, *Chem. Phys. Lett.*, 1985, **120**, 427.
- 22 N. Agamon, *Chem. Phys. Lett.*, 1995, **244**, 456.
- 23 K. D. Kreuer, *Solid State Ionics*, 1997, **94**, 55.